# LOCALIZED MODULUS OF ELASTICITY IN TIMBER AND ITS SIGNIFICANCE FOR THE ACCURACY OF MACHINE STRENGTH GRADING

*J. Oscarsson**†

Researcher
SP Wood Technology
SP Technical Research Institute of Sweden
Videum Science Park
SE-351 96 Växjö, Sweden
E-mail: jan.oscarsson@sp.se

*A. Olsson*

Professor
E-mail: anders.olsson@lnu.se

*B. Enquist*

Research Engineer
Department of Building and Energy Technology
Linnæus University
SE-351 95 Växjö, Sweden
E-mail: bertil.enquist@lnu.se

(Received February 2014)

**Abstract.** From previous research, it is well known that a localized modulus of elasticity (MOE) is a better indicating property (IP) of strength than an MOE averaged across a longer span. In this study, it was investigated to what extent the relationship, in terms of coefficient of determination ($R^2$), between strength and localized MOE was dependent on the length across which the MOE was determined. Localized MOE was calculated with MOE profiles based on dot laser scanning of fiber directions, axial dynamic excitation, and a scheme of integration across a board's cross-section. Two board samples were investigated. Maximum $R^2$ values, which were as high as 0.68 and 0.77, respectively, were obtained for localized MOE determined across lengths corresponding to about half the depth of the investigated boards. Consequently, application of a highly localized bending MOE as an IP will result in very competitive grading.

***Keywords:*** Fiber angle, indicating property, laser scanning, machine strength grading, modulus of elasticity, strain fields.

## INTRODUCTION

Machine strength grading of structural timber is based on statistical relationships between strength and various nondestructively measured wood characteristics such as density, annual ring width, stiffness in terms of modulus of elasticity (MOE), and occurrence of knots. Structural properties of timber are also influenced by *inter alia*, reaction wood, top ruptures, fiber angle, and fiber disturbances. From previous research (Hoffmeyer 1995), it is well known that the best single indicating property (IP) of strength in both bending and tension is MOE, which can be measured in different ways. The majority of commercial grading machines are based on either flatwise bending or axial dynamic excitation. In the first case, a bending test is carried out continuously as a timber member is passing through a machine. For most such machines, bending is obtained by a three-point loading test.

* Corresponding author
† SWST member

The length of span varies, typically between 600 and 1200 mm, depending on the make of the machine. The relationship between load, $P$, and deflection, $\delta$, is registered, and local static MOE ($E_{\mathrm{flat}}$) is determined as

$$E_{flat} = \frac{Pl^3}{48 I_{flat} \delta} \quad (1)$$

where $l$ is the span length and $I_{\mathrm{flat}}$ is the second moment of inertia in the flatwise direction. In connection with an axial dynamic excitation, a timber member is set into vibration by means of a hammer blow at one end. The resonance frequency of the first axial mode of vibration is determined on the basis of the impulse response captured by either a microphone or a laser vibrometer. The global (ie average) axial dynamic MOE ($E_{\mathrm{a,1}}$) is calculated as

$$E_{a,1} = 4\rho (f_{a,1} L)^2 \quad (2)$$

where $\rho$ is the board's mass density, $f_{\mathrm{a,1}}$ is the determined resonance frequency, and $L$ is the board length.

Another global MOE can be determined on the basis of resonance frequencies corresponding to edgewise (transversal) bending modes excited by a hammer blow on the board edge (Olsson et al 2012). Accurate calculation of edgewise bending MOE could be complicated, because bending vibrations include shear. However, shear deformations have a limited influence on resonance frequencies of lower bending modes. According to Bernoulli-Euler beam theory, in which shear deformations are disregarded, a bending MOE ($E_{\mathrm{b,1}}$) corresponding to the resonance frequency ($f_{\mathrm{b,1}}$) of the first edgewise bending mode can be estimated using

$$E_{b,1} = \frac{0.96 \rho L^4 f_{b,1}^2}{h^2} \quad (3)$$

where $h$ is the depth of the measured timber member (Fig 1). An approximation in accordance with Eq 3 will underestimate dynamic edgewise bending MOE by a few percent. A number of makes of grading machines based on bending excitation, flatwise and/or edgewise,

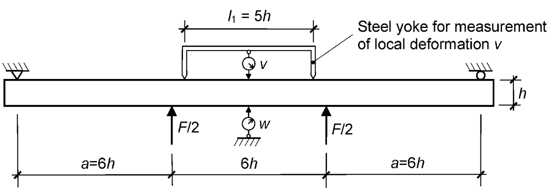


Figure 1. Test setup based on EN 408 (EN 2010b) for determining bending strength ($\sigma_{\mathrm{m}}$) and static edgewise bending modulus of elasticity (MOE), local ($E_{\mathrm{m,loc}}$) as well as global ($E_{\mathrm{m,glob}}$).

are approved for application on the European and North American market, respectively (Lanvin et al 2012; American Lumber Standard Committee 2013), but their share of each market is limited.

EN 408 (EN 2010b) specifies a test method for determining strength and local as well as global static MOE in edgewise bending. A test setup based on the standard is shown in Fig 1. The critical section, which according to EN 384 (EN 2010a) is defined as the section at which failure is expected to occur, shall be in a position between the two point loads. The local static edgewise MOE ($E_{\mathrm{m,loc}}$) is calculated as

$$E_{m,loc} = \frac{a l_1^2 (F_2 - F_1)}{16 I_e (v_2 - v_1)} \quad (4)$$

where $a = 6h$ is the distance from one of the point loads to the nearest support, $h$ is the depth of the timber member, $l_1$ is the length equal to $5h$ across which the local deformation $v$ is measured, $I_{\mathrm{e}}$ is the edgewise second moment of inertia, $F_2 - F_1$ is an increment of the sum of the two point loads, and $v_2 - v_1$ is the corresponding increment of local deformation. The global static edgewise MOE ($E_{\mathrm{m,glob}}$) is obtained from

$$E_{m,glob} = \frac{L_b^3 (F_2 - F_1)}{b h^3 (w_2 - w_1)} \left[ \left( \frac{3a}{4L_b} \right) - \left( \frac{a}{L_b} \right)^3 \right] \quad (5)$$

where $b$ is the member thickness, $L_{\mathrm{b}} = 18h$ is the span in bending, and $w_2 - w_1$ is the increment of global deformation.

EN 408 (EN 2010b) also includes a test method for determining both strength ($\sigma_{\mathrm{t,0}}$) and local

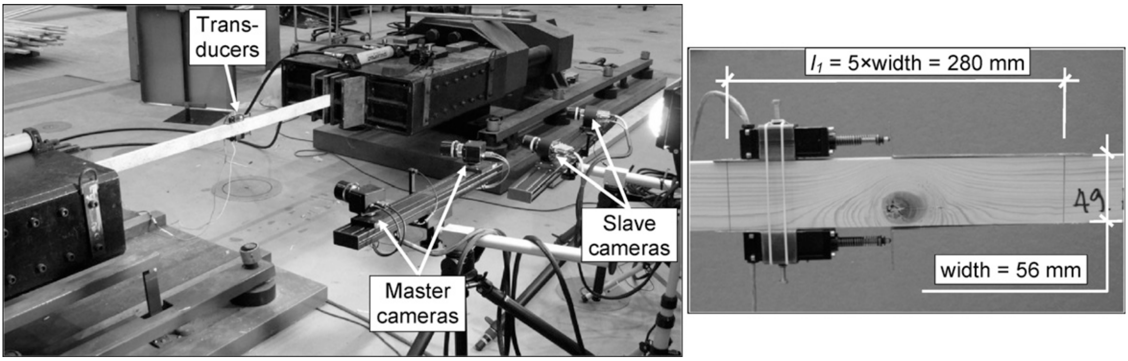


Figure 2. Setup for tension tests according to EN 408 (EN 2010b) and for digital image correlation measurements (left) and transducers for deformation measurements at assumed critical board section (right).

static MOE ($E_{t,0}$) in tension parallel to the grain. The latter is determined at the critical section as

$$E_{t,0} = \frac{l_1(F_2 - F_1)}{A(w_2 - w_1)} \tag{6}$$

where $A$ is the cross-sectional area, $F_2 - F_1$ is a load increment, and $w_2 - w_1$ is the corresponding increment of local deformation measured across a length ($l_1$) equal to five times the width (Fig 2, right).

In recent research (Olsson et al 2012; Oscarsson 2012), the MOE measures presented in Eqs 1-5 were determined for a sample of 105 strength-graded Norway spruce (Picea abies [L.] Karst.) planks of nominal dimensions 45 × 145 × 3600 mm sampled at Södra Timber's sawmill in Långasjö, Sweden. At the time of testing, the mean moisture content was 13%. The results presented in Table 1 show that the strongest relationship in terms of coefficient of determination ($R^2$) between bending strength and MOE was achieved for local static MOE in edgewise bending ($E_{m,loc}$) determined in accordance with the test setup shown in Fig 1. This relationship ($R^2 = 0.73$) was considerably stronger than those obtained for $E_{a,1}$, $E_{b,1}$, and $E_{flat}$, respectively, which, as described previously, are applied in commercial strength grading. Thus, the results in Table 1 indicate that more accurate strength grading would be achieved if grading methods based on IP reflecting localized edgewise MOE were available.

## Past Research

Previous research has shown that short-span MOE is a better IP of strength than long-span MOE. For example, the relationship between tension strength and flatwise bending MOE of Southern Pine (*Pinus* spp.) timber of different strength classes was investigated by Gerhards (1972) who found that $R^2$ was improved by 0.05 when the span length applied for determination of the bending MOE was decreased from

Table 1. Mean value, standard deviation (SD), relationship in terms of $R^2$ to bending strength ($\sigma_m$), and standard error of the estimate of $\sigma_m$ (SEE) for five different modulus of elasticity (MOE) measures (Eqs 1-5) obtained from investigating 105 planks of Norway spruce of nominal dimensions 45 × 145 × 3600 mm (Olsson et al 2012; Oscarsson 2012).[a]

| Method for assessment of MOE | Symbol | Mean (GPa) | SD (GPa) | $R^2$ between MOE and $\sigma_m$ | SEE (MPa) |
|---|---|---|---|---|---|
| Local static edgewise bending (EN 408 [EN 2010b]) | $E_{m,loc}$ | 11.0 | 2.8 | 0.73 | 6.8 |
| Global static edgewise bending (EN 408 [EN 2010b]) | $E_{m,glob}$ | 10.9 | 2.3 | 0.72 | 7.0 |
| Axial dynamic excitation | $E_{a,1}$ | 12.4 | 2.6 | 0.60 | 8.3 |
| Edgewise dynamic excitation | $E_{b,1}$ | 12.3 | 2.5 | 0.67 | 7.6 |
| Local static flatwise bending | $E_{flat}$ | 9.7 | 1.9 | 0.62 | 8.1 |

[a] Reported values are based on actual dimensions of 104 planks (one plank disregarded because of a major crack).

≈4570 to ≈1220 mm. Orosz (1976), who examined structural timber of west coast hemlock (*Tsuga heterophylla*), obtained optimum $R^2$ between tension strength and flatwise bending MOE when the latter was determined across a gage length of ≈406 mm.

For years, extensive research resources have been allocated to investigations concerning the possibility of determining MOE on a scale that is even more local than the one applied in EN 408 (EN 2010b). According to Bechtel et al (2006), the determination of MOE across a bending span such as the one applied in the determination of local MOE according to EN 408 (EN 2010b) or in grading machines based on three-point flatwise bending (author's remark) is a smoothing operation, which may mask the effect of knots and other local characteristics affecting structural value. The bending MOE, determined on the basis of applied bending forces and measured deflections across the span, is a composite result that represents the intrinsic MOE values at points along the length segment of the board coinciding with the bending span. Thus, the MOE value determined across such a span is a smoothed version of the underlying pointwise MOE values. Kass (1975) meant that a timber member exposed to bending may be considered as being composed of discrete regions, each with a distinct and individual (localized) bending stiffness. According to Foschi (1987), it is known that the correlation between strength and the smoothed MOE is improved if this MOE is replaced by the minimum localized MOE found within the measured span. The possibility of actually measuring the localized MOE across lengths that are much shorter than those applied in either EN 408 (EN 2010b) or in grading machines based on flatwise bending has been commented on by Kass (1975), Foschi (1987), Pope and Matthews (1995), and Aicher et al (2002). In these studies, it was emphasized that determination of local bending MOE across very short spans is a task that is associated with difficulties such as uncertainties related to accurate measuring of small deformations obtained across such spans. Another highlighted problem concerns occurrence of excessive stresses caused by beam bending or local crushing, the latter appearing at supports and load application points.

Other techniques developed to estimate bending MOE on a localized level have been presented. Boughton (1994) determined bending MOE in timber members using an edgewise four-point bending machine. MOE obtained on the basis of deformations measured across a span of 1200 mm was interpreted as an apparent MOE determined as a weighted moving average of the local stiffness properties within the span. The effects of this averaging were minimized using an algorithm by which the apparent MOE distribution along a member was used to calculate the corresponding localized edgewise MOE distribution. Application of an IP defined as the calculated minimum localized MOE found along a member resulted in predictions of strength in tension and edgewise bending that were more accurate than what was obtained using apparent MOE as IP. It was also shown that edgewise bending MOE was a better predictor of strength than flatwise bending MOE when both values were determined across the same span length.

The possibility of obtaining the true high-resolution distribution of MOE along timber members was also investigated by Bechtel (1985) and Foschi (1987). It was assumed that the relationship between MOE and strength would improve if the former was a true localized measure rather than an average value measured across a certain span. An approach that was originally presented by Bechtel (1985) was developed for application together with apparent MOE distributions determined by means of grading machines based on three-point flatwise bending. Basic features of the approach were the Fourier transform and weighting functions, the latter describing the fact that local MOE values near the center of a measurement span have a stronger influence on the measurement results than values at span ends. On the basis of the apparent MOE distribution and the weighting functions, the corresponding localized flatwise MOE distribution was to be calculated using the Fourier transform.

To test the approach, Foschi (1987) assumed three MOE distributions with different degrees of localization, determined the corresponding apparent distributions, and then reconstructed the localized distributions using the Fourier transform. It was found that both value and position of the true minimum MOE could be accurately predicted and that the apparent MOE distributions considerably overestimated the minimum MOE. The latter characteristic was also observed by Kass (1975). However, Foschi (1987) also found that determination of MOE distribution on the basis of deflections and loads related to short spans may be biased by measurement noise and numerical errors. Further investigation of this problem (Lam et al 1993) showed that the described approach would provide limited improvement of the correlation between strength and MOE compared with grading methods based on apparent MOE. Similar results were obtained by Pope and Matthews (1995).

Methods for stochastic modeling of localized MOE have also been developed. For example, Kline et al (1986) presented a model by which lengthwise variability in flatwise MOE could be generated with a resolution of 762 mm for two dimensions and two grades of Southern Pine (*Pinus* spp), and Taylor and Bender (1991) modeled localized flatwise MOE, with a resolution of 617 mm, for two grades and one dimension of Douglas fir (*Pseudotsuga menziesii*). The need for further research concerning improved measurement resolution and modeling of other species, grades, and board dimensions was pointed out in these studies.

## Objectives

The purpose of this study is to show how new measurement methods can be used for determining local MOE with high resolution and to identify suitable levels of localization of MOE when used as IP to bending strength. With laser scanning, it is now possible to determine local fiber orientation on wood surfaces with a resolution in the order of 1 mm along a timber member and in a speed corresponding to the production speed at a sawmill. In turn, knowledge of the fiber orientation enables the calculation of local MOE in the direction of the timber member and, by integration across the cross-section, also the bending stiffness or longitudinal stiffness on the corresponding scale along the member. Olsson et al (2013) suggested a novel IP to bending strength based on this approach. In this study, it was investigated to what extent $R^2$ between strength and local MOE was dependent on the length across which the MOE was determined and for which length an optimum relationship in terms of $R^2$ was achieved. In addition, it is shown how a contact-free measurement technique based on white-light digital image correlation (DIC) can be used to gain information concerning stiffness variation along the length of timber members. Thereby assumptions regarding the magnitude and significance of MOE in the close surroundings of knots, made by other researchers as previously described in the survey, are both verified and used in a new way.

# MATERIALS AND METHODS

## Materials

Test results obtained from two samples of timber, one of boards and one of planks, were used in this study. Both samples have been applied in previous but different studies. The plank sample was previously described and referred to in Table 1. The board sample consisted initially of 58 Norway spruce side boards of nominal dimensions 25 × 120 × 3900 mm. The boards, which were of saw-falling quality and sampled in a wet state, were planed and delivered to Linnæus University from the sawmill company Södra Timber, subsequently split and cut to nominal dimensions 25 × 56 × 3000 mm, and then used in a study concerning the possibility of grading narrow glulam laminations of Norway spruce side boards in a wet state using axial dynamic excitation (Oscarsson et al 2011). In that investigation, global axial dynamic MOE ($E_{a,1}$) and density ($\rho$) were determined both in a wet state and after drying to 12-14% MC. Local static MOE in tension ($E_{t,0}$) and tensile strength

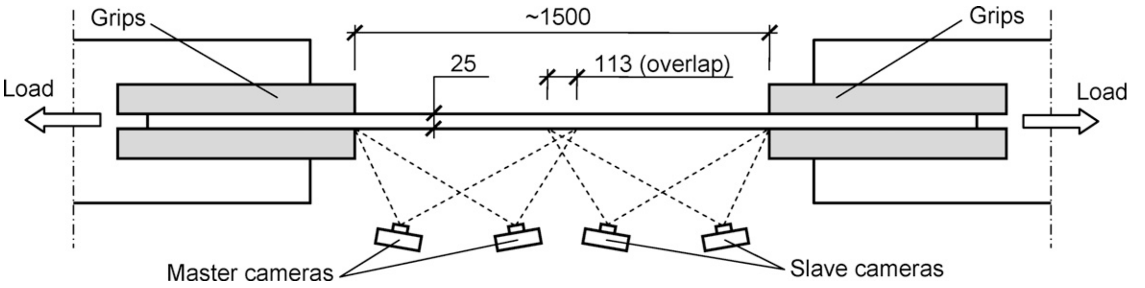


Figure 3. Camera setup (plan) for digital image correlation measurements.

Table 2. Mean value, standard deviation (SD), relationship in terms of $R^2$ to tension strength ($\sigma_{t,0}$), and standard error of the estimate of $\sigma_m$ (SEE) for three different modulus of elasticity (MOE) measures (Eqs 2 and 6) obtained from investigating 116 side boards of Norway spruce of nominal dimensions 25 × 56 × 3000 mm (Oscarsson et al 2011).[a]

| Method for assessment of MOE | Symbol | Mean (GPa) | SD (GPa) | $R^2$ between MOE and $\sigma_{t,0}$ | SEE (MPa) |
|---|---|---|---|---|---|
| Local static tension (EN 408 [EN 2010b])[b] | $E_{t,0}$ | 9.6 | 3.4 | 0.68 | 7.7 |
| Axial dynamic excitation, wet state[c] | $E_{a,1,wet}$ | 10.8 | 2.6 | 0.55 | 9.1 |
| Axial dynamic excitation, dried state[c] | $E_{a,1,dried}$ | 13.0 | 2.9 | 0.52 | 9.4 |

[a] Reported values are based on actual dimensions.
[b] Ten boards disregarded because of rot (eight) and damage (two).
[c] Eight boards disregarded because of rot.

($\sigma_{t,0}$) were determined in accordance with EN 408 (EN 2010b) after the dried boards had been stored at standard climate 20°C/65% RH for 7 mo. The tensile test setup is shown in Figs 2 and 3, and the relationships between stiffness measures and tensile strength are shown in Table 2. As for the plank sample, the largest $R^2$ was achieved for the locally determined static MOE.

## Tensile Tests and Strain Field Determination of Narrow Boards

For nine of the split boards included in the board sample, two-dimensional strain fields occurring on one of the flatwise surfaces during the tensile strength tests were determined on the basis of deformations measured by two contact-free measurement systems based on the DIC technique and connected in a master–slave fashion (Fig 2, left). The setup for the tensile tests and simultaneous DIC measurements is shown in Figs 2 and 3. The hydraulic testing machine had a 3.0-MN load cell. The distance between the wedge type grips was ≈1500 mm, and the load was applied with a constant loading rate of 7-8 kN/min. To ensure high measurement resolution of the long and narrow surface to be measured (56 × ≈1500 mm), two identical DIC ARAMIS systems (GOM mbH, Braunschweig, Germany) were used. Each system, including two cameras, separately measured deformations occurring on slightly more than half of the visible board length (Fig 3). Prior to the tests, two 3D coordinate systems, one for each DIC system, were defined through a calibration procedure carried out for each system and based on the cameras being positioned at angles and distances that depended on the size of the object to be measured. The difference in angle meant that stereoscopic photographs of the measured surface were obtained from each system. The master–slave application implied that photographs were taken simultaneously by both pairs of cameras at an interval of 3 s during a load test. Each such double pair of photographs represented a load stage to which unique strain fields corresponded. Based on the stereoscopic photographs, 3D positions (ie coordinates) of a large number of measurement points on the surface were determined for every load stage. The strains at each such point were calculated using the

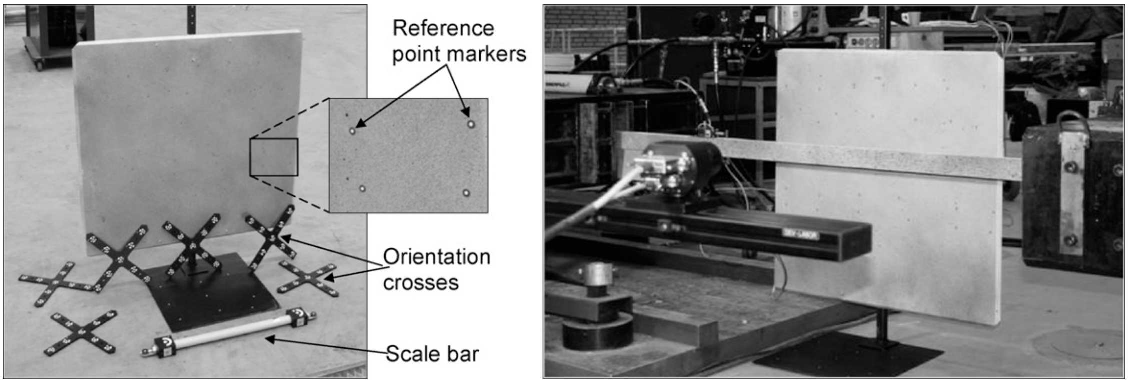


Figure 4. Setup for determining TRITOP coordinate system (left) and setup for establishing a relationship between ARAMIS coordinates and TRITOP coordinates.

ARAMIS software. The distance between measurement points was set to 3.6 mm in the longitudinal board direction and 1.8 mm in the lateral direction. Regarding the ARAMIS system, a more detailed description is found in Oscarsson et al (2012).

To be able to evaluate and visualize strains along the entire board length jointly and simultaneously, a third coordinate system to which the other two could be transformed was needed. For this purpose, yet another GOM measurement system called TRITOP was used. A setup (Fig 4, left) including orientation crosses, a scale bar, and 27 reference point markers fixed to a metal sheet, was arranged. On the basis of digital photographs of the setup taken from several angles using a photogrammetric camera, the third 3D coordinate system was defined using TRITOP software. This implied that the markers on the sheet shared a fixed TRITOP coordinate relationship, a characteristic that was used for the coordinate transformation. When a master–slave measurement was prepared, the sheet was put behind the board (Fig 4, right). As the photographs of the first load stage were taken, the markers were also caught and their positions in each ARAMIS coordinate system determined. With that, a relationship between TRITOP coordinates and ARAMIS coordinates was established and the transformation could be carried out accordingly. The transformed measurement results from the two ARAMIS systems were subsequently combined and jointly visualized (see Results and Discussion subsequently).

### Determination of Bending Modulus of Elasticity Profiles and Local Indicating Property

In the research referred to in Tables 1 and 2, the highest $R^2$ between strength and stiffness was achieved for edgewise and longitudinal MOE, respectively, determined locally on the basis of test setups described in EN 408 (EN 2010b). As previously described, it is known that more accurate grading will be achieved if grading methods based on locally determined edgewise IP are available and that such a method has recently been presented (Olsson et al 2013). In this new method, a commercial optical scanner of make WoodEye is applied for lengthwise dot laser scanning of timber surfaces. By means of the tracheid effect, high-resolution information about the angle φ between local fiber direction and the member's longitudinal direction is obtained (Fig 5a). Even small angles will cause considerable decrease of the structural properties, because wood is an orthotropic material with superior structural performance in the longitudinal fiber direction. Information about φ provides a basis for transformation of material properties related to the fiber direction to local material properties referring to the member's longitudinal direction. Local MOE in the latter

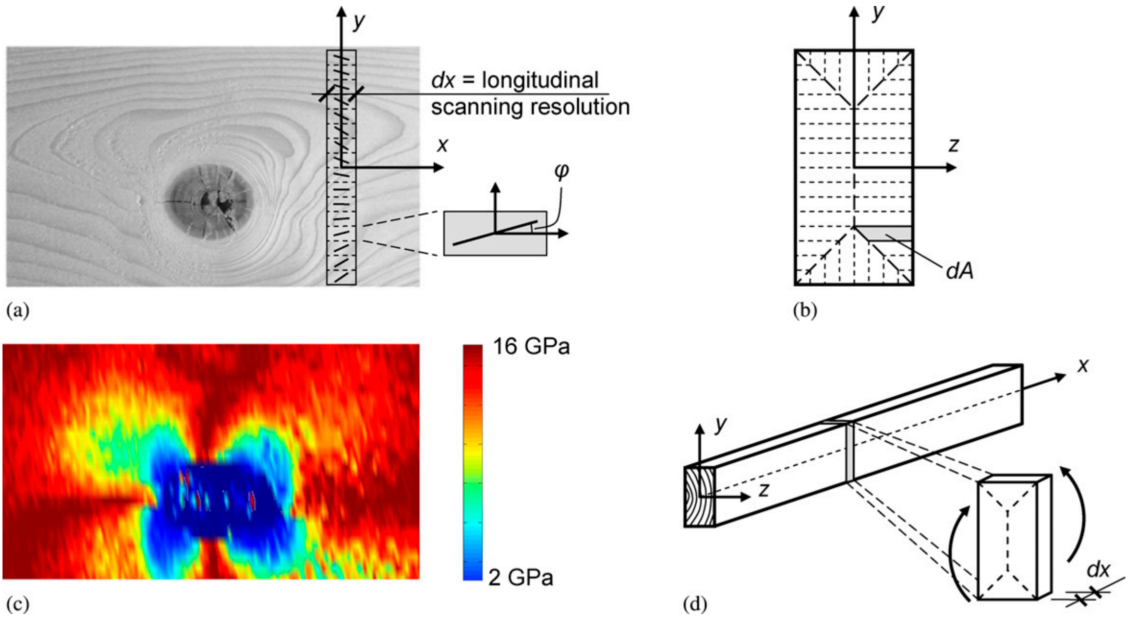


Figure 5. (a) Local fiber directions scanned on a member's surface by means of a row of laser dots, (b) cross-section divided into subareas implying that the exhibited angle φ and corresponding modulus of elasticity (MOE) in the member's longitudinal direction is valid within the volume $dA \times dx$, (c) distribution of longitudinal MOE around the exhibited knot, and (d) segment of length $dx$. The edgewise bending MOE of this segment was calculated by stiffness integration across the segment's cross section.

direction (Fig 5c) provides data for integration of MOE profiles valid for either edgewise bending or in the longitudinal direction of the member. According to Olsson et al (2013), the IP for a certain member is defined as the lowest edgewise bending MOE found along the member. Important assumptions used in the method presented by Olsson et al (2013) are that

- the Bernoulli-Euler beam theory is applicable,
- the density (ρ) and the MOE in the fiber direction ($E_l$) are constant within a member,
- an initial value of the MOE in the fiber direction ($E_{l,in}$) is assumed,
- other stiffness parameters are linear functions of $E_l$,
- fiber directions measured on the wood surface (Fig 5a) are located in the longitudinal–tangential plane,
- the fiber direction coincides with the wood surface, ie the diving angle is set to zero, and
- the fiber direction measured on a surface is valid to a certain depth. This means that the fiber angle φ highlighted in Fig 5a, and the corresponding local longitudinal MOE, is assumed to be valid within the volume defined by the area $dA$ (Fig 5b) times the length $dx$ (Figs 5a and 5d).

The only property, apart from ρ, that has to be determined individually for each member is $E_l$. To do this, the resonance frequency of the first axial mode of vibration ($f_{a,1}$) is measured and applied. The parameter $E_l$ is determined such that an axial eigenvalue analysis of a simple one-dimensional finite element model of the member, including an axial stiffness profile with the same shape as the one determined using the initially assumed value of $E_{l,in}$, results in the same longitudinal resonance frequency as the one determined experimentally.

The scanning resolution in the longitudinal direction, ie the distance between dot laser measurements, is dependent on the rate with which the members are fed through the scanner. In this study, in which the method presented by Olsson et al (2013) was applied, the feed rate was set to

60 m/min, resulting in a longitudinal scanning resolution of 0.8 mm. The resolution in the lateral direction is dependent on the configuration of the laser source. In this case, a source resulting in a lateral resolution of 4 mm was chosen.

## RESULTS AND DISCUSSION

### Digital Image Correlation Measurements

Results of DIC measurements can be exhibited using contour plots and section diagrams. A contour plot means that the strain distribution in longitudinal or lateral board direction or in shear is visualized for a certain load stage on the basis of a defined color scaling. Sections are defined in camera images as lines on the measured surface. Strains and displacements along such lines can be plotted in corresponding diagrams. An example (board no. 28B) of typically achieved results for the nine investigated boards is shown in Fig 6. The exhibited strains refer to a load stage at which the tensile stress had reached a value of 26.4 MPa, which is equivalent to 76% of the failure stress. This load stage was displayed because the contour plots for subsequent stages were disturbed by occurring cracks. An image of the measured surface is shown in Fig 6a. Contour plots showing longitudinal tensile strains ($\varepsilon_x$) achieved separately by the two DIC systems are exhibited in Fig 6b. The combination of these plots is shown in Fig 6c, which also includes the position of three defined sections and of the origin of the TRITOP coordinate system. Lateral (edgewise) displacements ($\Delta y$) along the defined sections are shown in Fig 6d, and longitudinal tensile strains ($\varepsilon_x$) along two of the sections are displayed in Fig 6e.

The most important result of the DIC measurements was that the decrease of MOE at critical knots occurred very locally. It was found that the length of such decrease, indicated in Fig 6e by the increase of longitudinal strain at TRITOP $x$-coordinates −650 and 350 mm, roughly corresponded to the board's width. This measure is just 20% of the length that according to EN 408 (EN 2010b) shall be applied for determining local MOE in tension (Eq 6). Thus, on the basis of the displayed results, it can be concluded that the method of EN 408 (EN 2010b) will overestimate local tensile MOE at critical knots, because the stipulated measurement length of 280 mm (Fig 2, right) will include clear wood parts in which the stiffness is unaffected by the presence of knots. In this context, knots are of particular importance, because failures in timber members are very often related to such defects (Johansson 2003). The described overestimation of localized MOE was also observed by Foschi (1987), who noted that determination of an apparent flatwise bending MOE across a span of 910 mm would overestimate the true minimum MOE and by Kass (1975) who found that the edgewise MOE of a defect zone was overestimated by an amount that is dependent on the length of this zone, the span length across which deformations are measured, and the ratio of MOE of the defect region to the MOE of surrounding clear wood material.

Another observation that can be made from the DIC measurements is that considerable displacements in the edgewise board direction, ie perpendicular to the load direction, occur (Fig 6d). Because displacement peaks coincide with major edge knots, a reasonable explanation is that these displacements can be attributed to uneven stress distribution across the cross-section.

### Bending Modulus of Elasticity Profiles and Relationship between Indicating Property and Bending Strength

Typical edgewise bending MOE profiles obtained for one of the members in the investigated plank sample are shown in Fig 7. The left profile exhibits a bending MOE profile calculated for maximum resolution, ie a resolution equal to the scanning resolution. The right profile displays a moving average MOE calculated across an interval equal to half the depth of the member. The latter means that each MOE value along the profile is calculated as the average value of the surrounding 72 mm, ie along 36 mm on each side of the longitudinal position in question. A comparison of the two graphs shows

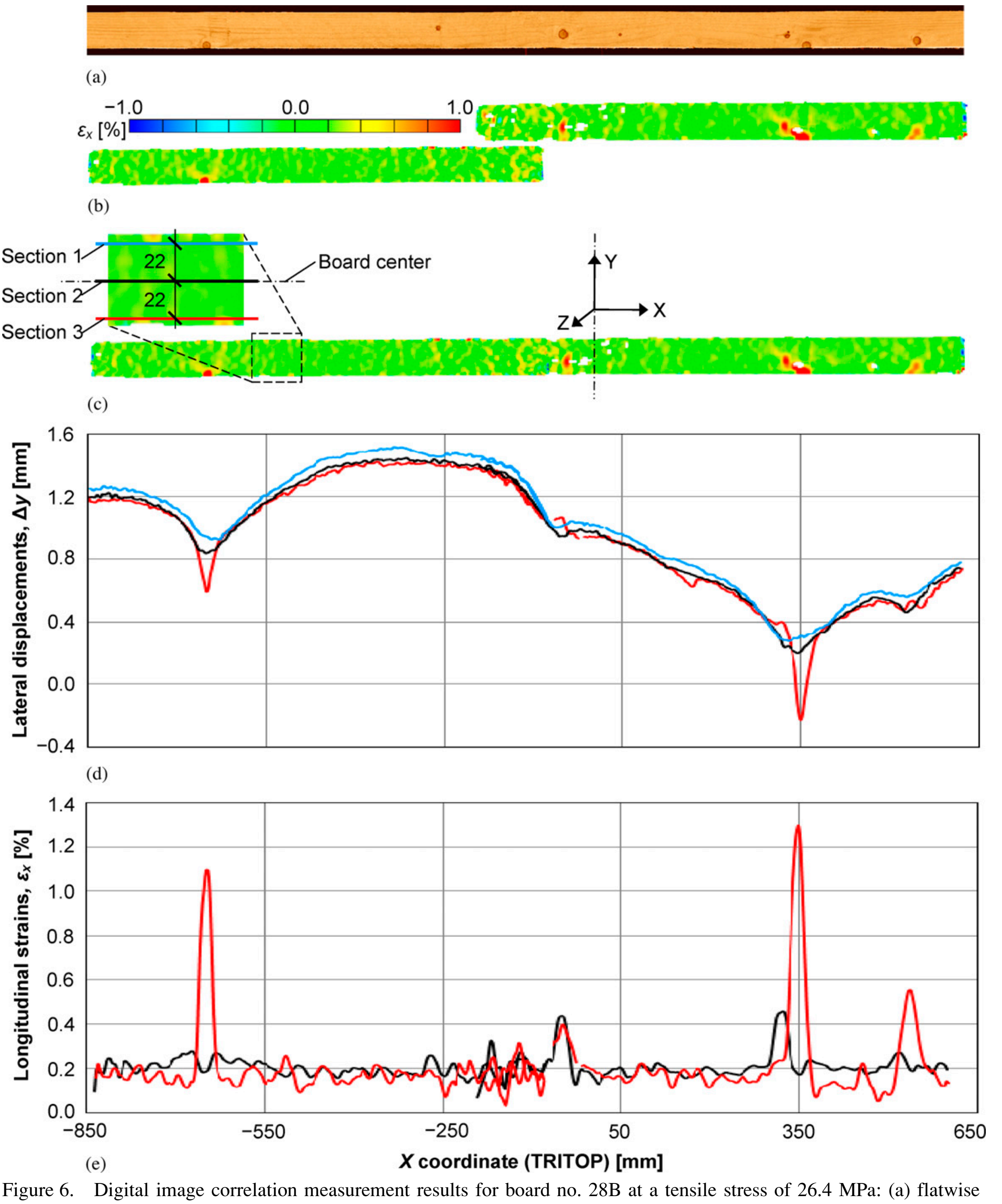


Figure 6. Digital image correlation measurement results for board no. 28B at a tensile stress of 26.4 MPa: (a) flatwise board surface; (b) contour plots of longitudinal strains, $\varepsilon_x$, determined by master system (left) and slave system (right); (c) combined contour plot, positions of defined sections (left detail), and position of TRITOP coordinate system (right detail); (d) displacements, $\Delta y$, in edgewise board direction along Sections 1-3; and (e) longitudinal strains, $\varepsilon_x$, along Sections 2-3.

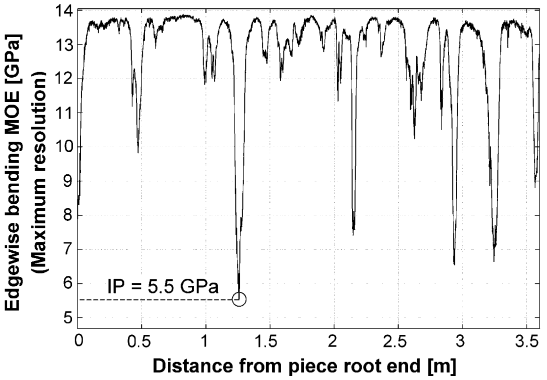


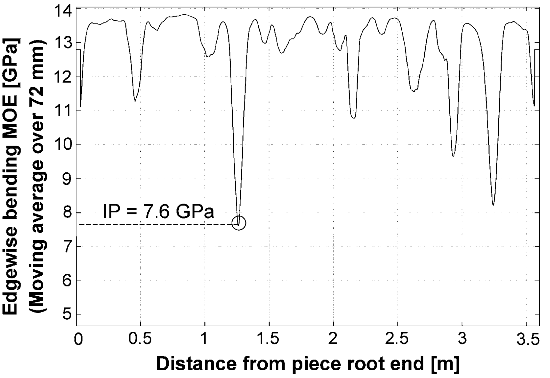


Figure 7. Bending modulus of elasticity (MOE) profiles for plank no. 34 corresponding to maximum scanning resolution (left) and to a moving average calculated across a length interval of half the depth of the plank (right), respectively (IP, indicating property).

that the dependency of the IP on the length of the moving average interval is strong. The IP corresponding to full resolution was 5.5 GPa, whereas a higher value (IP = 7.6 GPa) was reached for the moving average profile. The relationship between IP and length interval of moving average was studied in more detail. Of particular interest was the IP achieved for the interval of 725 mm, equal to five times the depth, ie the length across which local MOE in both bending and tension is determined according to EN 408 (EN 2010b). This IP was as high as 12.0 GPa, whereas the actual local edgewise bending MOE according to EN 408 (EN 2010b) was 10.6 GPa. The results are in accordance with research referred to in the Past Research section regarding the overestimation of pointwise MOE values because of smoothing effects when MOE is averaged across a span of certain length. Of particular interest is the considerable difference between the pointwise MOE = 5.5 GPa obtained at maximum scanning resolution (Fig 7, left) and the corresponding local MOE = 10.6 GPa achieved on the basis of EN 408 (EN 2010b).

For the board sample, profiles of both bending and axial MOE were studied and corresponding IP in terms of lowest MOE along each board was determined. As for the planks, the dependency of the IP on the length of the moving average interval was noted. Consequently, it was also interesting to investigate to what extent the variation of length interval influenced the $R^2$ between IP and strength. For both samples, MOE profiles of bending and axial MOE, respectively, were calculated for different length intervals and corresponding IPs were determined. The results presented in Fig 8 show that, for both samples, higher $R^2$ was achieved for IP based on bending. For the board sample, which was tested in tension, this may be surprising, but an explanation may be that edge knots cause uneven stress distribution across the cross-section resulting in edgewise deformations, as discussed in connection with the edgewise deformations exhibited in Fig 6d. The results in Fig 8 also show that maximum $R^2$ values were, for the planks loaded in bending, achieved for an IP determined across a length interval of about 90 mm and, for the boards loaded in tension, for an IP determined across a length interval of about 25 mm. These lengths correspond to about half the depth of each type of member. They also correspond to the typical length of clusters of knots or to the diameter of individual critical knots, respectively, at the sections in which failure occurs in each type of member. A comparison between these $R^2$ values and those presented in Tables 1 and 2 reveals interesting facts, partly discussed in Olsson et al (2013). The maximum $R^2 = 0.68$ for the plank sample (Fig 8, left) is higher than those referring to $E_{a,1}$, $E_{b,1}$, and $E_{flat}$ in Table 1, implying that the new grading method presented in Olsson et al (2013) can provide a grading accuracy that exceeds what is achieved by common methods

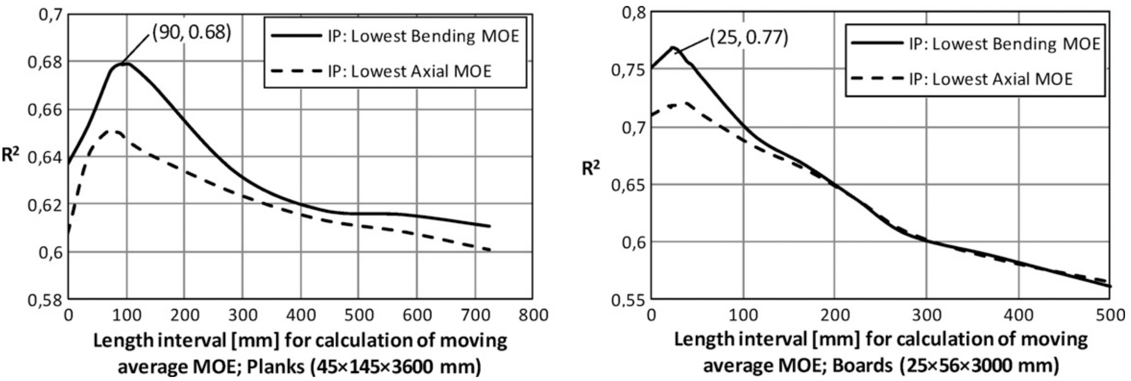


Figure 8. Relationship between length interval for calculating moving average modulus of elasticity (MOE_ and $R^2$ between strength and indicating property (IP) (IP determined as lowest edgewise bending MOE and lowest axial MOE, respectively).

on the market. However, $R^2$ determined on the basis of static edgewise bending MOE according to EN 408 (EN 2010b) ($E_{\mathrm{m,loc}}$ and $E_{\mathrm{m,glob}}$ in Table 1) is stronger than 0.68. Because MOE was determined on the basis of the standard reflect "real" MOE, it can be concluded that there is a potential for improvement with regard to the assumptions on which the new strength grading method is based. For example, it is likely that inclusion of the diving angle would improve the performance of the new method. Analysis of results from contact-free deformation measurements has also shown that local deformations occurring within knot clusters cannot be properly described by means of beam theory. Yet the maximum $R^2 = 0.77$ for the board sample (Fig 8, right) was remarkably strong compared with those presented in Table 2, which was probably because of the fact that the strength of narrow pieces is much more dependent on the occurrence of single large knots and that this characteristic is properly caught by means of the new method.

## CONCLUSIONS

The research presented in this study shows and quantifies what has been assumed but only partly verified by other researchers, namely that determination of local MOE on the basis of EN 408 (EN 2010b) hides the effect of localized defect zones and, consequently, results in an overestimation of local MOE on the scale most relevant for prediction of strength. By application of a new strength grading method (Olsson et al 2013) in which MOE profiles are applied for IP determination, it is shown that maximum $R^2$ between strength, in bending as well as in tension, and IP is achieved for IP determined as moving average bending MOE calculated across a length interval of approximately half the depth of investigated timber members. The application of fiber orientation information obtained by means of dot laser scanning for calculation of MOE on a closer scale is still quite new, and further development of the approach towards even more accurate predictions of stiffness and strength can be foreseen.

## REFERENCES

Aicher S, Höfflin L, Behrens W (2002) Determination of local and global modulus of elasticity in wooden boards. Otto-Graf-Journal 13:183-198.

American Lumber Standard Committee (2013) List of approved machines. ALSC, Germantown, MD. http://www.alsc.org/untreated_machinegraded_mod.htm (21 November 2013).

Bechtel FK (1985) Beam stiffness as a function of pointwise E, with application to machine stress rating. *In* Proc International Symposium on Forest Products Research, CSIR, Pretoria, South Africa.

Bechtel FK, Hsu CS, Wang N, Hanshaw TC (2006) Method for estimating compliance at points along a beam from bending measurements. US Patent 7.047.156 B1.

Boughton G (1994) Superior sorting of timber using localised stiffness on edge. Pages 510-515 *in* Jodie Wells, ed. Proc Pacific Timber Engineering Conference, 11-15 July 1994, Gold Coast, Australia. Timber Research and

Development Advisory Council, Fortitude Valley, Queensland, Australia.

EN (2010a) EN 384 Structural timber—Determination of characteristic values of mechanical properties and density. European Committee for Standardization, Brussels, Belgium.

EN (2010b) EN 408 Timber structures—Structural timber and glued laminated timber – Determination of some physical and mechanical properties. European Committee for Standardization, Brussels, Belgium.

Foschi RO (1987) A procedure for the determination of localized modulus of elasticity. Holz Roh Werkst 45(6):257-260.

Gerhards CC (1972) Relationship of tensile strength of Southern pine dimension lumber to inherent characteristics. Res Pap FPL-174. USDA For Serv Forest Prod Lab, Madison, WI.

Hoffmeyer P, ed (1995) Strength grading adds value, Part 2—Available technique. Technical University of Denmark, Lyngby, Denmark. Technical Report 335-1995 [in Danish, Norwegian, and Swedish].

Johansson C-J (2003) Grading of timber with respect to mechanical properties. Pages 23-43 *in* S Thelandersson and HJ Larsen, eds. Timber engineering. John Wiley & Sons, Ltd., Chichester, UK.

Kass AJ (1975) Middle ordinate method measures stiffness variation within pieces of lumber. Forest Prod J 25(3):33-41.

Kline DE, Woeste FE, Bendtsen BA (1986) Stochastic model for modulus of elasticity of lumber. Wood Fiber Sci 18(29):228-238.

Lam F, Foschi RO, Barrett JD, He QY (1993) Modified algorithm to determine localized modulus of elasticity of lumber. Wood Sci Technol 27(2):81-94.

Lanvin J-D, Reuling D, Rouger F (2012) Machines for classification of wood according to strength: Presentation of different measurement techniques for grading French species (document updated 1 November 2012). FCBA Institut Technologique, Paris, France [in French].

Olsson A, Oscarsson J, Johansson M, Källsner B (2012) Prediction of timber bending strength on basis of bending stiffness and material homogeneity assessed from dynamic excitation. Wood Sci Technol 46(4):667-683.

Olsson A, Oscarsson J, Serrano E, Källsner B, Johansson M, Enquist B (2013) Prediction of timber bending strength and in-member cross-sectional stiffness variation on the basis of local wood fibre orientation. Eur J Wood Products 71(3):319-333.

Orosz I (1976) Relationship between apparent modulus of elasticity, gage length, and tensile strength of lumber. Wood Sci Technol 10(4):273-291.

Oscarsson J (2012) Strength grading of structural timber and EWP laminations of Norway spruce—Development potentials. Licentiate thesis, Report No. 15. School of Engineering, Linnæus University, Växjö, Sweden. 131 pp.

Oscarsson J, Olsson A, Enquist B (2012) Strain fields around knots in Norway spruce specimens exposed to tensile forces. Wood Sci Technol 46(4):593-610.

Oscarsson J, Olsson A, Johansson M, Enquist B, Serrano E (2011) Strength grading of narrow dimension Norway spruce side boards in the wet state using first axial resonance frequency. International Wood Products Journal 2(2):108-114.

Pope DJ, Matthews FW (1995) A comparison of deconvolution techniques to improve MOR estimation from stress grading machine output. Wood Sci Technol 29(6):431-439.

Taylor SE, Bender DA (1991) Stochastic model for localized tensile strength and modulus of elasticity in lumber. Wood Fiber Sci 23(4):501-519.